# MONTE-CARLO SIMULATIONS OF DISORDERED NON-EQUILIBRIUM PHASE TRANSITIONS

by

Mark Dickison

A THESIS

Presented to the Faculty of the Graduate School of the

UNIVERSITY OF MISSOURI–ROLLA

in Partial Fulfillment of the Requirements for the Degree

MASTER OF SCIENCE IN PHYSICS

2005

Approved by

Thomas Vojta, Advisor

Gerald Wilemski

David Grow

# ABSTRACT

This thesis focuses on the effects of both correlated and non-correlated disorder on non-equilibrium phase transitions, specifically those found in the d-dimensional contact process. These effects are studied by means of extensive Monte-Carlo simulations. The scaling behavior of various parameters is evaluated for both cases, and the results are compared with theory. For the correlated disorder case, the stationary density in the vicinity of the transition is also examined, and found to be smeared.

The behavior in both cases can be understood as the results of rare regions where the system is locally free of disorder. For point-like defects, i.e., uncorrelated disorder, the rare regions are of finite size and cannot undergo a true phase transition. Instead, they fluctuate slowly which gives rise to Griffiths effects. In contrast, if the rare regions are infinite in at least one dimension, a stronger effect occurs: each rare region can independently undergo the phase transition and develop a nonzero steady state density. This leads to a smearing of the global transition.

## ACKNOWLEDGMENT

I would first like to thank Dr. Thomas Vojta, for his help, guidance, and inspiration. This thesis would not have been possible without him.

I would also like to thank Dr.Gerald Wilemski, and Dr. David Grow, for taking the time out of their busy schedule to judge this, as well as for invaluable instruction they have provided over the years.

Finally, I'd like to thank my family and friends, you know who you all are, for sticking with me through all these years.

# TABLE OF CONTENTS

Page

ABSTRACT . . . . . iii

ACKNOWLEDGMENT . . . . . iv

LIST OF ILLUSTRATIONS . . . . . vii

LIST OF TABLES . . . . . viii

SECTION

1. INTRODUCTION . . . . . 1
   - 1.1. The Contact Process . . . . . 3
     - 1.1.1. Absorbing States . . . . . 4
     - 1.1.2. Non-Equilibrium Phase Transitions . . . . . 4
     - 1.1.3. Connections to Directed Percolation . . . . . 5
   - 1.2. Disorder Effects . . . . . 8
     - 1.2.1. Harris Criterion . . . . . 8
     - 1.2.2. Griffiths Effects . . . . . 9
     - 1.2.3. Disorder Induced Smearing . . . . . 10
2. MONTE-CARLO SIMULATIONS OF THE SMEARED PHASE TRANSITION IN A CONTACT PROCESS WITH EXTENDED DEFECTS 2005 *Jour. Phys. A* **38** 1199 . . . . . 12
   - 2.1. Abstract . . . . . 12
   - 2.2. Introduction . . . . . 12
   - 2.3. Theory . . . . . 15
     - 2.3.1. Contact process with extended impurities . . . . . 15
     - 2.3.2. Smeared phase transition . . . . . 16
   - 2.4. Monte-Carlo simulations . . . . . 19
     - 2.4.1. Simulation method . . . . . 19
     - 2.4.2. Time evolution . . . . . 20
     - 2.4.3. Stationary state . . . . . 22
   - 2.5. Conclusions . . . . . 24
3. POINT-LIKE DISORDER IN A CONTACT PROCESS . . . . . 27
   - 3.1. Simulations and Results . . . . . 28
   - 3.2. Conclusions . . . . . 32
4. Conclusions . . . . . 34

APPENDICES

A. PROGRAMMING IMPLEMENTATION AND SOURCE CODE . . . . 36

BIBLIOGRAPHY . . . . . 47

VITA . . . . . 49

# LIST OF ILLUSTRATIONS


| Figure | | Page |
|---|---|---|
| 1.1 | Illustration of Percolation and Directed Percolation | 6 |
| 2.1 | Overview of the time evolution of the density $\rho$ | 20 |
| 2.2 | Left: Logarithm of the density at the clean critical point, Right: Decay constant $E$ of the stretched exponential | 21 |
| 2.3 | Approach of the density to its nonzero stationary value in the tail of the smeared transition | 22 |
| 2.4 | Stationary density $\rho_{st}$ as a function of birth rate | 23 |
| 2.5 | Left: Logarithm of the stationary density $\rho_{st}$, Right: Decay constant $B$ as a function of $-\ln(1-p)$. | 24 |
| 3.1 | Logarithm of the density at the clean critical point | 29 |
| 3.2 | Finding $\lambda_c$ | 30 |
| 3.3 | $\rho^{-1/\delta}$ vs $\ln t$ for $p = 0.2, \ldots, 0.5$ | 31 |
| 3.4 | Left: Time evolution of single site survival probability Right: Time evolution of single site cluster size | 32 |
| 3.5 | Time dependence of the density in the Griffiths region | 33 |

# LIST OF TABLES

Table Page

1.1 Critical exponents and associated quantities for d-dimensional directed percolation . . . . . 7

# 1. INTRODUCTION

In nature, thermal equilibrium is more of an exception than the rule. Nonequilibrium systems dominate our daily lives, from weather patterns to chemical reactions to the spreading of disease. While many aspects of nonequilibrium systems are unusual and different from equilibrium systems, there are some properties that are shared between the two cases, such as phase transitions. In recent years, phase transitions between different nonequilibrium states have become a topic of great interest. A prominent class of nonequilibrium phase transitions separates active fluctuating states from inactive absorbing states where fluctuations cease entirely[1]. These absorbing state transitions have applications ranging from physics to chemistry to biology[1, 2, 3, 4]. The generic universality class for absorbing state transitions is directed percolation[5].

A prototypical member of the directed percolation universality class is the contact process[1, 6]. To provide a biological model, imagine a forest of elm trees, some of which are infected with Dutch elm disease. The infection spreads to nearby trees with the rate $\lambda$ and is healed at unit rate. It is intuitively clear that for a low enough infection rate the infection will die out, and likewise, for a high enough rate there will be a nonequilibrium steady state density of infected trees. Mathematically speaking, the contact process consists of a $d$-dimensional hypercubic lattice. Each site can be vacant or occupied. During the time evolution, particles duplicate themselves and spread to their nearest neighbors at rate $\lambda$, and are annihilated at unit rate. For small $\lambda$, annihilation dominates and the absorbing state with no occupied sites is the only steady state. For large $\lambda$ there is a steady state with finite particle density (active phase). The two phases are separated by a nonequilibrium phase transition at $\lambda = \lambda_c^0$. Section 1.1 will discuss these concepts in deeper detail.

In a realistic system, the spreading and recovery rates will not be constant, but will vary from site to site. For the biological model, this can be interpreted in many ways: geographical factors making neighbors less likely to become infected, a locally less virulent strain of the disease, etc. From analogy to similar equilibrium phase transitions[7], one would initially expect that the sharp phase transition survives with only a shift in the value of $\lambda_c$. However, Thomas Vojta[8] has shown that this belief is in general not true. He developed a theory which predicts that disorder correlated in a sufficient number of dimensions can destroy a sharp continuous phase transition and smear it over a parameter interval. The system divides itself into separate regions which essentially act as independent and can become active at different values of the control parameter $\lambda$. The biological analogy would be a forest separated by cliffs, valleys, and mountain ranges. Unlike conventional phase transitions where the entire system is either in its ordered or in its disordered phase, strongly correlated impurities make different parts of the system undergo the phase transition independently of each other. The phase transition is therefore smeared and the order develops very inhomogeneously. A more in depth discussion of these phenomena can be found in Section 1.2.

In contrast, for pointlike disorder, different parts of the system cannot undergo the phase transition independently. Therefore the transition is predicted to be sharp, but with logarithmically slow time dynamics.

The goal of this thesis is to analyze the results of large-scale Monte-Carlo simulations of the contact process with both correlated and non-correlated disorder in order to test these predictions. Section 2 discusses simulations of a two-dimensional contact process model with linear defects (correlated disorder) and short-range interactions. The system consists of a $2d$ square lattice with as many as several million sites, each of which can be occupied or empty. The correlated disorder is simulated by introducing parallel lines of weak duplication rate, i.e., lines with $\lambda(\vec{r}) = c\lambda$, where

$c < 1$. The results of the simulations show that the phase transition is indeed destroyed and smeared over a range of $\lambda$. Order develops very inhomogeneously, i.e., the rare regions devoid of impurities become active first, while the bulk system is still in the inactive phase. As $\lambda$ is lowered more of these rare regions become active and eventually the system becomes completely active. Unlike in the case of a continuous phase transition, in our case activity develops independently on different parts of the system. The dynamics close to the smeared transition is very slow, showing stretched-exponential or even power-law time-dependent decay of the density. The numerical results are in good agreement with the initial predictions[8].

In Section 3, the effects of non-correlated, or pointlike, disorder are examined. A sharp phase transition is found, in agreement with predictions. While previous research[9] had shown non-universal behavior, this thesis shows that for long enough time scales, the system possesses universal behavior just as expected at a critical point, but with exponential scaling, rather than the usual power-law scaling. In order to explore these very long time scales, it was necessary to switch to a $1d$ lattice, however the results can be extended to higher dimensions.

Finally, in Section 4, these results and simulations will be summarized and brought to a conclusion.

## 1.1. THE CONTACT PROCESS

As mentioned above, the system of interest to this thesis is the contact process[1, 6]. The specific implementation of the contact process used here involved a d-dimensional hypercubic lattice. At any given point in time each site is associated with either a 0, representing an unoccupied site, or a 1, representing an occupied site. The system is allowed to evolve in time by picking a single occupied site at random, and selecting either creation, at probability $\lambda/(\lambda + 1)$ or annihilation at probability $1/(\lambda + 1)$, where $\lambda$ is a nonnegative parameter. If creation is selected, one of the

$2N$ nearest neighbors is selected at random. If it is unoccupied, its value is set to 1. If annihilation is selected, the chosen site's value is set to 0. In either case, time is advanced by $1/N_p$, where $N_p$ is the total number of infected individuals. While the original contact process is a process in continuous time, in order to implement the Monte Carlo simulation, it is necessary to discretize the process. This method was initially proposed by Dickman[10].

This system has many notable features. Of interest to this investigation is the fact that it possesses a non-equilibrium transition between an active and an absorbing state, as well as its similarities and connections to Directed Percolation.

1.1.1. Absorbing States The absorbing state transition discussed in the introductory paragraph is difficult to explain quantitatively, but fairly trivial to explain in a qualitative manor. Consider the $2d$ contact process again. Since the growth rate is proportional to the number of occupied nearest neighbors, it is clear that if the system ever enters into a state where no sites are occupied, the growth rate will then be zero for all sites, and the system will never leave the empty inactive state. Such a state, that can be entered but never left, is referred to as an "absorbing state". As was mentioned before, for values of $\lambda$ small compared to the annihilation rate, one expects the system to enter the absorbing state in the long time limit. The biological analogy would say that an insufficiently virulent disease will eventually die out. On the other hand, for values of $\lambda$ large compared to the annihilation rate, one of course expects occupied sites to survive. Much like the flu, a virulent disease is generally suffered by some relatively constant fraction of the population. Thus there is an active steady state for high $\lambda$, and an absorbing steady state for low $\lambda$. This suggests that there may be a phase transition between these two states as $\lambda$ is varied.

1.1.2. Non-Equilibrium Phase Transitions It must be emphasized that all the steady states discussed above are non-equilibrium states that cannot be characterized by a Boltzmann distribution $e^{-\beta E}$. In fact, the contact process does not even allow

the notion of energy. Thus all the traditional, thermodynamic, methods of analyzing phase transitions will not work. Luckily, though non-equilibrium phase transitions arise out of a fundamentally different class of states, they still share many of the same characteristics of continuous equilibrium phase transitions[1]. Both types of phase transitions are associated with a control parameter $\lambda$ crossing a critical value $\lambda_c$. In addition, behavior near critical points can be described according to power law scaling of the form

$$X_n = |\lambda - \lambda_c|^n \tag{1.1}$$

where $X_n$ is an observable specific to the system, (heat capacity for thermodynamic phase transitions, magnetization for magnetic models), and $n$ is a universal critical exponent associated with that particular observable. Many quantities have expressions of this form, with only the value of $n$ changing. These are universal exponents in that they do not vary based on the microscopic details of the system, but only macroscopic qualities such as the dimensionality of the system, and any symmetries it might have. Those details define universality classes, which are groups of systems that share the same critical exponents.

1.1.3. Connections to Directed Percolation It has been previously asserted that the contact process is a member of the directed percolation universality class[1, 6]. In order to show that this is the case, it is easiest to consider a geometrical or graphical representation. In Figure 1.1, an example of the $2d$ directed percolation problem can be seen. Bonds are formed randomly along the lattice paths with some probability $\lambda$, and directed percolation is achieved if a path can be achieved from the bottom to the top without ever going downward. If the up-down direction is interpreted as a temporal dimension, rather than a spatial dimension, and bonds are considered to represent particle duplication or site infection; it is easily seen that the survival probability of a contact process is analogous to the probability of a path forming

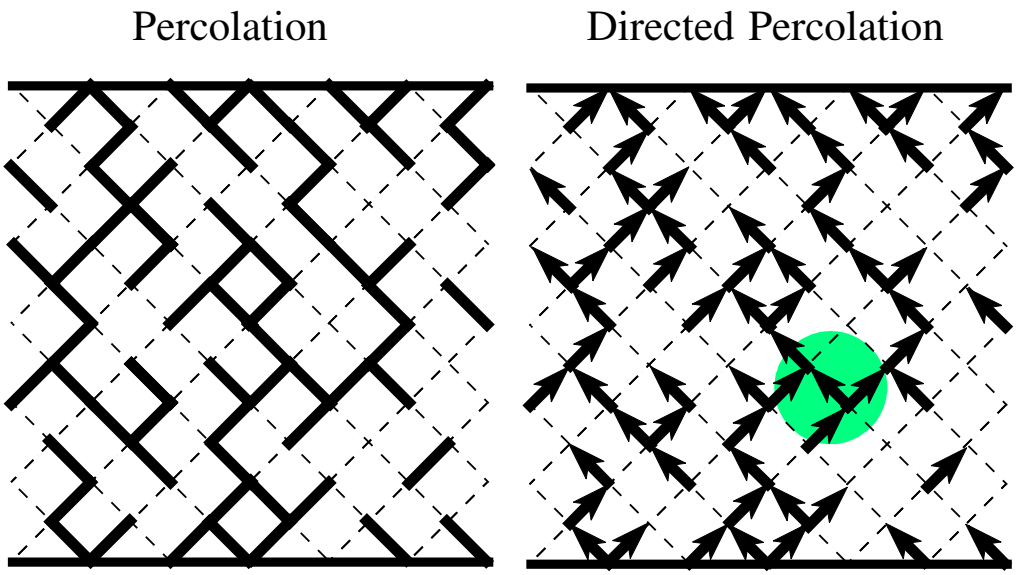


Figure 1.1. Illustration of Percolation and Directed Percolation. Percolation is achieved if an unbroken line is formed from bottom to top. In Directed percolation, only paths that advance along the direction of the arrows are considered.

for the directed percolation problem. As such, they will have exactly the critical exponents, and as such, belong to the same universality class. Table 1.1 lists values of the critical exponents for the directed percolation universality class. $\beta$ is the critical exponent associated with the steady state density $\rho$ , which is the long time limit of the proportion of occupied sites, with defining equation

$$\rho = (\lambda - \lambda_c)^{\beta}. \tag{1.2}$$

$\nu_{\perp}$ and $\nu_{\parallel}$ are the exponents of the correlation lengths in the space and time dimensions respectively, and are associated with the typical size of a cluster in the respective

Table 1.1. Critical exponents and associated quantities for d-dimensional directed percolation[1]

| Critical Exponent | d=1 | d=2 | d=3 |
|---|---|---|---|
| $\beta$ | 0.276486 | 0.584 | 0.81 |
| $\nu_\perp$ | 1.096854 | 0.734 | 0.581 |
| $\nu_\parallel$ | 1.733847 | 1.295 | 1.105 |
| $z$ | 1.580745 | 1.76 | 1.90 |
| $\delta$ | 0.159464 | 0.451 | 0.73 |
| $\theta$ | 0.313686 | 0.230 | 0.12 |

dimensions. The relevant equations are

$$\begin{aligned} \xi_\perp &= (\lambda - \lambda_c)^{\nu_\perp}, \\ \xi_\parallel &= (\lambda - \lambda_c)^{\nu_\parallel}. \end{aligned} \tag{1.3}$$

$z$ is the ratio between $\nu_\perp$ and $\nu_\parallel$, and leads to the equation

$$\xi_t = \xi^z. \tag{1.4}$$

Lastly $\delta$ describes the survival probability at the critical point $\lambda = \lambda_c$ of a cluster starting from a single site, as well as the time evolution of the density starting from a full lattice. $\theta$ is associated with number of sites in a cluster that started from a single site. These time dependent equations are of the form

$$\begin{aligned} P_s(t) &= t^{-\delta}, \\ \rho(t) &= t^{-\delta}, \\ N(t) &= t^{\theta}. \end{aligned} \tag{1.5}$$

## 1.2. DISORDER EFFECTS

The results discussed in the previous section assume that the control parameter associated with the system is spatially homogenous, with no changes in its value as one moves from point to point within the system. However in the real world such ideal conditions are often impossible to realize[11]. Thus the question arises of what happens when some form of disorder is introduced into the system. Three questions that immediately arise about the behavior of the phase transition are are: 1) Does the phase transition remain sharp? 2) If so, does it have the same critical behavior as the clean transition, or do the critical exponents or even the character of the scaling relations change? And 3) Is the behavior still universal?

Quenched, i.e. time-independent, disorder is perhaps the most common type, and is the easiest to realize. The effects of quenched disorder on directed percolation have been examined before, by several researchers, and the results were very inconclusive. Renormalization group analysis, a common technique to analyze critical point behavior, showed only runaway solutions towards large disorder[12], indicating unusual behavior. In addition, simulations produced results that indicated the critical exponents were non-universal[13, 14, 15, 16], with no explanation as to why. To find answers to the above questions is very important, and the Harris criterion can provide a partial answer to the first two.

### 1.2.1. Harris Criterion

The Harris Criterion[13, 17] is a general rule relating the critical exponent of the spatial correlation length $\nu_\perp$ to the effects of quenched disorder on critical points. It states that if the correlation length critical exponent of the clean transition fulfills the inequality $\nu_\perp \geq 2/d$ where $d$ is the spatial dimensionality, then the disorder does not affect the behavior of the system at the critical point, and the same power law behavior with the same exponents will occur, though

with a shift in the non-universal value of $\lambda_c$. Table 1.1 illustrates that the relevant quantity, $\nu_\perp$, violates the Harris criterion for all listed $d$. When the Harris criterion is violated, generally, the result is a new critical point with the same sort of power law scaling discussed in Section 1.1.2, but with new exponents which allow it to fulfill the Harris criterion. In some rare cases, however, other, more interesting behavior can be observed; this behavior depends on how the disorder changes at large length scales.

Two general classes can be defined if the Harris criterion is violated, but a sharp transition still exists[18]. In the first class[19, 20], the disorder remains noticeable at all length scales, with the relative strength of the disorder approaches some finite value as the length scale increases arbitrarily. In this case, the generic result occurs as discussed above, the system retains power-law scaling with new exponents that allow it to fulfill the Harris criterion. In the second class however, disorder effects increase without limit on large length scales[21]. The conventional power law scaling is lost, and is replaced by activated, i.e. exponential, scaling. In addition, the probability distributions of macroscopic quantities become very broad even on a logarithmic scale, with their width diverging with increasing system size. Consequently, events which would normally be exponentially rare can come to dominate average behavior. In the renormalization group formulation, these critical points with infinite disorder are referred to as infinite-randomness critical points, and their general behavior is discussed below in brief. Realization of these points is shown in Section 3.

1.2.2. Griffiths Effects While the previous sections have only considered the global nature of the disorder, Griffiths phenomena depend on the local effects of rare strong spatial disorder fluctuations. These fluctuations can affect not only the critical point itself, but the vicinity around it. In the region between $\lambda_c$, the dirty critical point, and $\lambda_c^0$, the clean critical point, the bulk system is in the absorbing phase. However, in an infinite sized sample, there is an exponentially small, but nonzero probability for finding an arbitrarily large spatial region devoid of impurities. These

rare regions, known as Griffiths islands, can be locally active while the rest of the system is in the absorbing phase. The dynamics associated with these Griffiths islands are very slow, because changing state requires a coherent change of the order parameter over this arbitrarily large region. The presence of these locally active islands produces an essential singularity in many observables in the region between $\lambda_c$ and $\lambda_c^0$[22], which is often called the Griffiths phase. While in generic classical equilibrium systems, this behavior has not been observed, due to weakness of these effects, in quantum systems, or classical systems with correlated disorder, the Griffiths effects become strong enough to be observed in experiments[21]. In some such systems, the Griffiths effects can become strong enough to destroy the phase transition entirely, which is known as smearing[23], and will be discussed in the next paragraph.

1.2.3. Disorder Induced Smearing Previously, it has been assumed that the phase transition remains sharp in the presence of quenched disorder. It can be shown however, that in some systems the rare region effects can become so strong that the phase transition is completely destroyed by smearing. Consider a single rare region that is locally in the active phase. In the generic case of uncorrelated disorder this region is of finite extension. Therefore it cannot undergo a true phase transition independently of the bulk system. The slow fluctuations of this rare region thus lead to the Griffiths effects[22] discussed in Section 1.2.2. However, the reliance of this effect on the fluctuation of the phase of the rare regions suggest that if these regions are capable of undergoing true phase transitions then the behavior of the system as a whole could completely change. Recent work has shown that this sort of local phase transition does indeed occur in disordered quantum systems[23] or classical systems with correlated disorder[24]. This changes the behavior of the system, leading to a smeared global phase transition.

These smeared transitions exhibit notably different behavior from a conventional sharp transition. At a conventional transition, the ordered phase develops as a global

feature of the entire system. This transition is signified by a diverging correlation length of the order parameter fluctuations at the critical point, and by singularities in the accompanying observables. In contrast, in these smeared transitions, the system divides itself up into spatial regions which independently undergo the phase transition at different values of the control parameter. Global order thus develops very irregularly over a range of control parameter values. The correlation length remains finite, the singularities of observables are rounded, and the sharp transition is destroyed.

In the contact process with extended quenched defects, rare regions are infinite in the correlated dimensions, but finite in the random directions. Since the contact process displays a phase transition already in one dimension, the phase transition in this system can happen independently on these rare regions, as such, we expect to see a smeared transition in this system. Computational verification of this is provided in Section 2.

In contrast, for point-like defects, these rare regions are not infinite in any direction, and thus an active phase cannot develop independently on them. In this case the transition remains sharp, and one of the aforementioned infinite randomness fixed points arises, which leads to activated scaling of the form $\xi_{\parallel} \sim \exp(\xi_{\perp}^{\mu})$. However, contrary to previous predictions[9], this is indeed universal behavior in the long time limit. Computational verification of this is provided in Section 3.

# 2. MONTE-CARLO SIMULATIONS OF THE SMEARED PHASE TRANSITION IN A CONTACT PROCESS WITH EXTENDED DEFECTS [1]

Mark Dickison and Thomas Vojta

*Department of Physics, University of Missouri - Rolla, Rolla, MO 65409, USA*

## 2.1. ABSTRACT

We study the nonequilibrium phase transition in a contact process with extended quenched defects by means of Monte-Carlo simulations. We find that the spatial disorder correlations dramatically increase the effects of the impurities. As a result, the sharp phase transition is completely destroyed by smearing. This is caused by effects similar to but stronger than the usual Griffiths phenomena, viz., rare strongly coupled spatial regions can undergo the phase transition independently from the bulk system. We determine both the stationary density in the vicinity of the smeared transition and its time evolution, and we compare the simulation results to a recent theory based on extremal statistics.

## 2.2. INTRODUCTION

Rare regions are an important, if intricate, aspect of systems with impurities and defects. In recent years, their influence on phase transitions and critical phenomena has reattracted considerable attention. Rare region effects were first studied in the context of classical equilibrium phase transitions. Griffiths [22] showed that they lead to a singular free energy in an entire parameter region in the vicinity of the phase transition, now known as the Griffiths region. However, in classical systems with

[1] THE TEXT OF THIS SECTION HAS BEEN PUBLISHED AS A RESEARCH PAPER IN 2005 *JOUR. PHYS. A* **38** 1199

uncorrelated disorder, this Griffiths singularity in the free energy is an essential one and thus very weak and probably unobservable in experiment. Disorder correlations generically increase the effects of impurities. Therefore, stronger rare region effects have been found in classical systems with extended defects and in random quantum systems (where the correlations are in imaginary time direction). In the random transverse field Ising model [25], or equivalently, the classical McCoy-Wu model [26], the Griffiths singularity takes a power law form, accompanied by a diverging magnetic susceptibility in the Griffiths region. Very recently, it has been found that some phase transitions can even be completely destroyed by smearing when the rare regions order independently from the bulk system. This happens, e.g., in a classical Ising magnet with planar defects [27] and in itinerant quantum ferromagnets [23].

In this paper, we investigate the effects of rare regions on *nonequilibrium* phase transitions with quenched spatial disorder. We concentrate on the prominent class of absorbing state phase transitions which separate active, fluctuating states from inactive, absorbing states where fluctuations cease entirely [2, 3, 1, 4]. The generic universality class for absorbing state transitions is directed percolation (DP) [5]. According to a conjecture by Janssen and Grassberger [28], all absorbing state transitions with a scalar order parameter, short-range interactions, and no extra symmetries or conservation laws belong to this class. Examples include the transitions in the contact process [29], catalytic reactions [30], interface growth [31], or turbulence [32].

The effects of *uncorrelated* spatial disorder, i.e., point-like defects, on the DP transition have been studied in some detail in the past. According to the Harris criterion [17, 13], the DP universality class is unstable against spatial disorder, because the (spatial) correlation length exponent $\nu_\perp$ violates the inequality $\nu_\perp > 2/d$ for all spatial dimensionalities $d < 4$. Indeed, in the corresponding field theory, spatial disorder leads to runaway flow of the renormalization group (RG) equations [12], destroying the DP behavior. Several other studies [15, 14, 33, 16] agreed on the

instability of DP against spatial disorder, but a consistent picture has been slow to evolve. Recently, Hooyberghs *et al.* applied the Hamiltonian formalism [34] to the contact process with spatial disorder [9]. Using a version of the Ma-Dasgupta-Hu strong-disorder RG [35] these authors showed that the transition (at least for sufficiently strong disorder) is controlled by an exotic infinite-randomness fixed point with activated rather than the usual power-law scaling.

Very recently, it has been suggested [8] that extended spatial defects like dislocations, disordered layers, or grain boundaries can have an even more dramatic effect on nonequilibrium phase transitions in the DP universality class. Rare region effects similar to but stronger than the usual Griffiths phenomena [22, 13] actually destroy the sharp transition by smearing. This happens because rare strongly coupled spatial regions can undergo the transition independently from the bulk system. Based on an extremal statistics approach it has been predicted [8] that the spatial density distribution in the tail of the smeared transition is very inhomogeneous, with the average stationary density and the survival probability depending exponentially on the control parameter.

In the present paper we present results of extensive Monte-Carlo simulations of a two-dimensional contact process with linear spatial defects which provide numerical evidence for this smearing scenario in a realistic model with short-range couplings. The paper is organized as follows. In section 2.3., we introduce the model and briefly summarize the results of the extremal statistics theory for the smeared phase transition. In section 2.4. we present our simulation method and the numerical results together with a comparison to the theoretical predictions. We conclude in section 2.5. by discussing the importance of our results and their generality.

## 2.3. THEORY

### 2.3.1. Contact process with extended impurities

The contact process [29] is a prototypical system in the directed percolation universality class. It can be interpreted, e.g., as a model for the spreading of a disease. The contact process is defined on a $d$-dimensional hypercubic lattice. Each lattice site $\mathbf{r}$ can be active (occupied by a particle) or inactive (empty). During the time evolution, active sites can infect their neighbors or they can spontaneously become inactive. Specifically, particles are created at empty sites at a rate $\lambda n/(2d)$ where $n$ is the number of active nearest neighbor sites and the 'birth rate' $\lambda$ is the control parameter. Particles are annihilated at unit rate. For small birth rate $\lambda$, annihilation dominates, and the absorbing state without any particles is the only steady state (inactive phase). For large birth rate $\lambda$, there is a steady state with finite particle density (active phase). The two phases are separated by a nonequilibrium phase transition in the DP universality class at $\lambda = \lambda_c^0$.

Quenched spatial disorder can be introduced by making the birth rate $\lambda$ a random function of the lattice site. Point-like defects are described by spatially uncorrelated disorder. We are interested in the case of extended defects which can be described by disorder perfectly correlated in $d_c$ dimensions, but uncorrelated in the remaining $d_r = d - d_c$ dimensions. Here $d_c = 1$ and 2 corresponds to linear and planar defects, respectively. Thus, $\lambda$ is a function of $\mathbf{r}_r$ which is the projection of the position vector $\mathbf{r}$ on the uncorrelated directions. For definiteness, we assume that the birthrate values $\lambda(\mathbf{r}_r)$ are drawn from a binary probability distribution

$$P[\lambda(\mathbf{r}_r)] = (1-p)\,\delta[\lambda(\mathbf{r}_r) - \lambda] + p\,\delta[\lambda(\mathbf{r}_r) - c\lambda] \tag{2.1}$$

where $p$ and $c$ are constants between 0 and 1. In other words, there are extended impurities of spatial density $p$ where the birth rate $\lambda$ is reduced by a factor $c$.

2.3.2. Smeared phase transition

In this subsection, we briefly summarize the arguments leading to the smearing of the phase transition and the predictions of the extremal statistics theory [8] to the extent necessary for the comparison with the Monte-Carlo results.

In analogy to the Griffiths phenomena [22, 13], there is a small but finite probability $w$ for finding a large spatial region of linear size $L_r$ (in the uncorrelated directions) devoid of impurities. Up to pre-exponential factors, this probability is given by

$$w \sim \exp(-\tilde{p} L_r^{d_r}) \tag{2.2}$$

with $\tilde{p} = -\ln(1-p)$. These rare regions can be locally in the active phase, even if the bulk system is still in the inactive phase. Since the impurities in our system are extended, each rare region is infinite in $d_c$ dimensions but finite in the remaining $d_r$ dimensions. This is a crucial difference to systems with uncorrelated disorder, where the rare regions are finite. In our system, each rare region can therefore undergo a true phase transition *independently* of the rest of the system at some $\lambda_c(L_r) > \lambda_c^0$. According to finite-size scaling [36],

$$\lambda_c(L_r) - \lambda_c^0 = A L_r^{-\phi} \ , \tag{2.3}$$

where $\phi$ is the clean ($d$-dimensional) finite-size scaling shift exponent and $A$ is the amplitude for the crossover from a $d$-dimensional bulk system to a 'slab' infinite in $d_c$ dimensions but but finite in $d_r$ dimensions. If the total dimensionality $d = d_c + d_r < 4$, hyperscaling is valid, and $\phi = 1/\nu_\perp$ which we assume from now on.

The resulting global phase transition is very different from a conventional continuous phase transition, where a nonzero order parameter develops as a collective

effect of the entire system, accompanied by a diverging correlation length in all directions. In contrast, in our system, the order parameter develops very inhomogeneously in space with different parts of the system (i.e., different $\mathbf{r}_r$ regions) ordering independently at different $\lambda$. Correspondingly, the correlation length in the uncorrelated directions remains finite across the transition. This defines a smeared transition.

In order to determine the global system properties in the vicinity of the smeared transition, we combine (2.2) and (2.3) to obtain the probability for finding a rare region which becomes active at $\lambda_c$ as

$$w(\lambda_c) \sim \exp\left(-B(\lambda_c - \lambda_c^0)^{-d_r\nu_\perp}\right) \tag{2.4}$$

for $\lambda_c - \lambda_c^0 \to 0+$. Here, $B = \tilde{p}A^{d_r\nu_\perp}$.

The total density $\rho$ (the total number of active sites) at a certain $\lambda$ is obtained by summing over all active rare regions, i.e., all regions with $\lambda > \lambda_c$. Since the functional dependence on $\lambda$ of the density on any given active island is of power-law type it does not enter the leading exponentials but only the pre-exponential factors. Thus, the stationary density develops an exponential tail,

$$\rho_{st}(\lambda) \sim \exp\left(-B(\lambda - \lambda_c^0)^{-d_r\nu_\perp}\right) \ , \tag{2.5}$$

for all birth rates $\lambda$ above the clean critical point $\lambda_c^0$. Analogous arguments can be made for the survival probability $P(\lambda)$ of a single seed site. If the seed site is on an active rare region it will survive with a probability that depends on $\lambda$ via a power law. If it is not on an active rare region, the seed will die. To exponential accuracy the survival probability is thus also given by (2.5). The local spatial density distribution in the tail of the smeared transition is very inhomogeneous. On active rare regions, the density is of the same order of magnitude as in the clean system. Away from these regions it is exponentially small.

We now turn to the dynamics in the tail of the smeared transition. The long-time decay of the density (starting from a state with $\rho = 1$) is dominated by the rare regions while the bulk contribution decays exponentially. According to finite size scaling [36], the behavior of the correlation time $\xi_t$ of a single rare region of size $L_r$ in the vicinity of the clean bulk critical point can be modelled by

$$\xi_t(\Delta, L_r) \sim L_r^{(z\nu_\perp - \tilde{z}\tilde{\nu}_\perp)/\nu_\perp} \left|\Delta - AL_r^{-1/\nu_\perp}\right|^{-\tilde{z}\tilde{\nu}_\perp} \quad . \tag{2.6}$$

Here $\Delta = \lambda - \lambda_c^0 > 0$, $z$ is the $d$-dimensional bulk dynamical critical exponent, and $\tilde{\nu}_\perp$ and $\tilde{z}$ are the correlation length and dynamical exponents of a $d_r$-dimensional system. To exponential accuracy, the time dependence of the total density is given by

$$\rho(\lambda, t) \sim \int dL_r \ \exp\left[-\tilde{p}L_r^{d_r} - Dt/\xi_t(\Delta, L_r)\right] \tag{2.7}$$

where $D$ is a constant.

Let us first consider the time evolution at the clean critical point $\lambda = \lambda_c^0$. For $\Delta = 0$, the correlation time (2.6) simplifies to $\xi_t \sim L_r^z$. Using the saddle point method to evaluate the integral (2.7), we find the leading long-time decay of the density to be given by a stretched exponential,

$$\ln \rho(t) \sim -\tilde{p}^{z/(d_r+z)} \ t^{d_r/(d_r+z)} \ . \tag{2.8}$$

For $\lambda < \lambda_c^0$, i.e, in the absorbing phase, the correlation time of the largest islands does not diverge but is cut-off by the distance from the clean critical point, $\xi_t \sim \Delta^{-z\nu}$. The large islands with this correlation time dominate the variational integral (2.7). This leads to a simple exponential decay with a decay constant $\tau \sim \Delta^{-z\nu}$

The most interesting case is $\lambda > \lambda_c^0$, i.e., the tail region of the smeared transition. Here, we repeat the saddle point analysis with the full expression (2.6) for

the correlation time. For intermediate times $t < t_x \sim (\lambda - \lambda_c^0)^{-(d_r+z)\nu_\perp}$ the decay of the average density is still given by the stretched exponential (2.8). For times larger than the crossover time $t_x$ the system realizes that some of the rare regions are in the active phase and contribute to a finite steady state density. The approach of the average density to this steady state value is characterized by a power-law.

$$\rho(t) - \rho(\infty) \sim t^{-\psi} \ . \tag{2.9}$$

The value of $\psi$ cannot be found by our methods since it depends on the neglected nonuniversal pre-exponential factors.

## 2.4. MONTE-CARLO SIMULATIONS

### 2.4.1. Simulation method

We now illustrate the smearing of the phase transition by extensive computer simulation results for a 2d contact process with linear defects ($d_c = d_r = 1$). There is a number of different ways to actually implement the contact process on the computer (all equivalent with respect to the universal behavior). We follow the widely used algorithm described, e.g., by Dickman [10]. Runs start at time $t = 0$ from some configuration of occupied and empty sites. Each event consists of randomly selecting an occupied site $\mathbf{r}$ from a list of all $N_p$ occupied sites, selecting a process: creation with probability $\lambda(\mathbf{r}_r)/[1 + \lambda(\mathbf{r}_r)]$ or annihilation with probability $1/[1 + \lambda(\mathbf{r}_r)]$ and, for creation, selecting one of the neighboring sites of $\mathbf{r}$. The creation succeeds, if this neighbor is empty. The time increment associated with this event is $1/N_p$.

Using this algorithm, we have performed simulations for linear system sizes up to $L = 3000$ and impurity concentrations $p = 0.2, 0.25, 0.3, 0.35$ and $0.4$. The relative strength of the birth rate on the impurities was $c = 0.2$ for all simulations. The data presented below represent averages of 200 disorder realizations. We have chosen

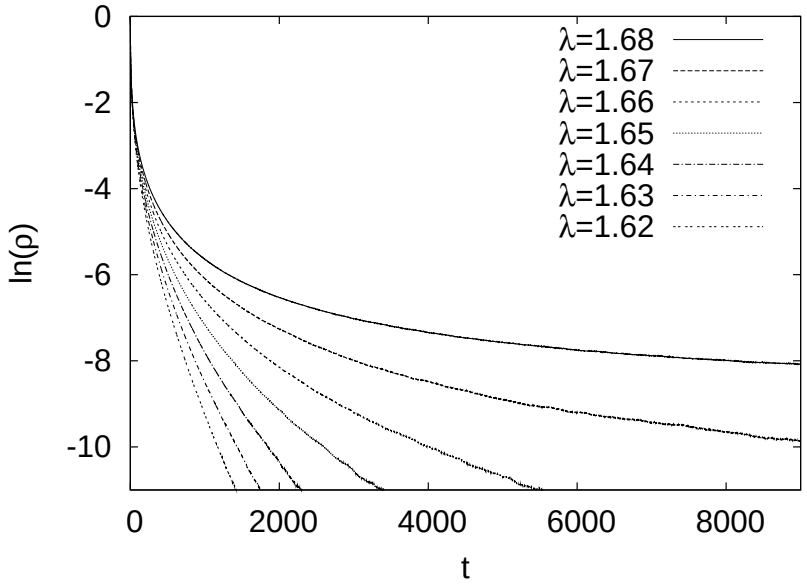


Figure 2.1. Overview of the time evolution of the density $\rho$ for a system with $L = 3000$ and $p = 0.2$ and several birth rates ($\lambda = 1.68, \ldots, 1.62$ from top to bottom) in the vicinity of the clean critical point $\lambda_c^0 = 1.6488$.

these parameters, viz., a low concentration of impurities which have a birth rate much smaller than the bulk, because these conditions are favorable for observing the smeared transition in a finite size simulation. If $p$ was too large, the exponential drop-offs in eqs. (2.5) and (2.8) would be very steep and hard to observe over a significant range of $\lambda$ or $t$, respectively. If $c$ was too close to one, clean critical fluctuations would mask the tail of the smeared transition.

2.4.2. Time evolution

In this subsection, we discuss the time evolution of the density starting from a completely occupied lattice, $\rho(0) = 1$. Figure 2.1 presents an overview of the behavior of a system with impurity concentration $p = 0.2$, system size $L = 3000$, and several birth rates from $\lambda = 1.62 \ldots 1.68$. The clean critical point is at $\lambda_c^0 = 1.6488$ [14]. The figure shows that the long-time decay of the density in the absorbing phase, $\lambda < \lambda_c^0$, is approximately exponential, in agreement with the expectation discussed after eq.

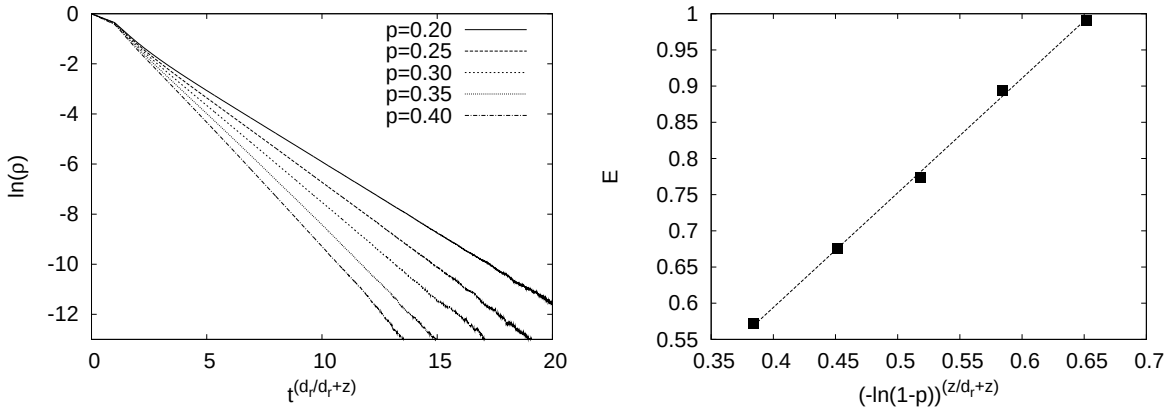


Figure 2.2. Left: Logarithm of the density at the clean critical point $\lambda_c^0$ as a function of $t^{d_r/(d_r+z)} = t^{0.362}$ for several impurity concentrations ($p = 0.2, \ldots, 0.4$ from top to bottom) and $L = 3000$. The long-time behavior follows a stretched exponential $\ln \rho = -Et^{0.362}$. Right: Decay constant $E$ of the stretched exponential as a function of $[-\ln(1-p)]^{z/(d_r+z)} = [-\ln(1-p)]^{0.638}$.

(2.8) The decay constant of this exponential increases with decreasing $\lambda$. In contrast, for $\lambda > \lambda_c^0$ the density approaches a nonzero value in the long-time limit. Close to $\lambda_c^0$, the density appears to decay, but slower than exponentially.

According to eq. (2.8), the behavior right at the clean critical point, $\lambda = \lambda_c^0$, is expected to be a stretched exponential rather than a simple exponential decay. To shed more light on the time evolution at $\lambda_c^0$, the behavior of $\ln \rho$ as a function of $t^{d_r/(d_r+z)}$ is presented in the left panel of figure 2.2 for several impurity concentrations $p$. For our system, $d_r/(d_r + z) = 0.362$ with $z = 1.76$ being the dynamical exponent of the clean 2d contact process [37]. The figure shows that the data follow a stretched exponential behavior $\ln \rho = -Et^{0.362}$ over more than three orders of magnitude in $\rho$, in good agreement with eq. (2.8). (The very slight deviation of the curves from a straight line can be attributed to the pre-exponential factors neglected in the extremal statistics theory). The right panel of figure 2.2 shows the decay constant $E$, i.e., the slope of these curves as a function of $\tilde{p} = -\ln(1-p)$. In good approximation, the values follow the power law $E \sim \tilde{p}^{z/(d_r+z)} = \tilde{p}^{0.638}$ predicted in (2.8).

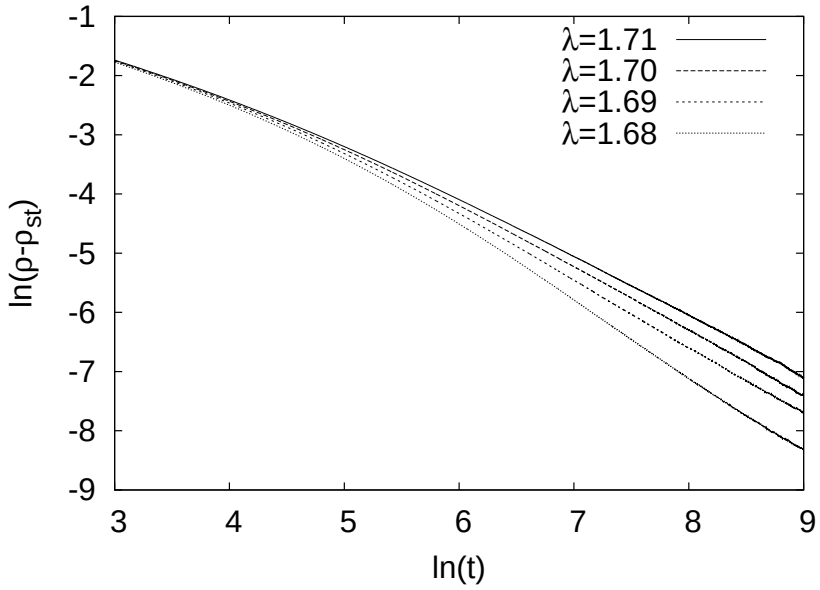


Figure 2.3. Double-logarithmic plot of the approach of the density to its nonzero stationary value in the tail of the smeared transition for a system with $p = 0.2$ and $L = 3000$ and birth rate $\lambda = 1.71, 1.70, 1.69, 1.68$ (top to bottom). The long-time behavior is of power-law type, $(\rho(t) - \rho_{st}) \sim t^{-\psi}$. Fits yield exponents of approximately 1.00, 1.08, 1.12, and 1.28, respectively.

In the tail of the smeared transition, i.e. for $\lambda > \lambda_c^0$ the density has a constant nonzero value $\rho_{st} = \rho(\infty)$ in the long-time limit. Figure 2.3 illustrates the approach of the density to this value. It shows $\ln[\rho(t) - \rho_{st}]$ as a function of $\ln(t)$ for several $\lambda$. The long-time behavior is clearly of power-law type, but the exponent depends on $\lambda$, i.e., it is nonuniversal. These results agree with the corresponding prediction in eq. (2.9).

2.4.3. Stationary state

In this subsection we present and analyze the simulation results for the stationary state in the tail of the smeared transition, $\lambda > \lambda_c^0$. Figure 2.4 shows a comparison of the stationary density $\rho_{st}$ as a function of $\lambda$ between the clean system and a dirty system with $p = 0.2$. The clean system ($p = 0$) has a sharp phase transition with a power-law singularity of the density, $\rho_{st} \sim (\lambda - \lambda_c^0)^\beta$ with $\beta \approx 0.58$ in agreement with

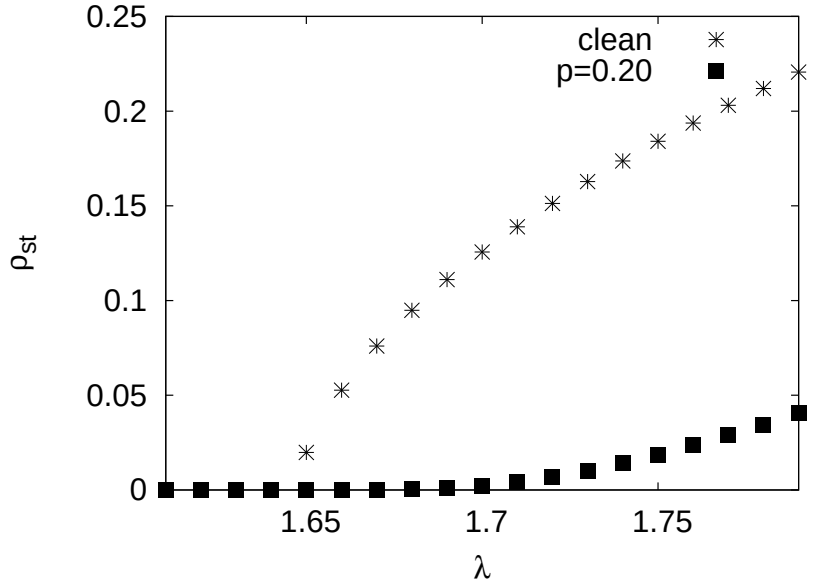


Figure 2.4. Stationary density $\rho_{st}$ as a function of birth rate $\lambda$ for a clean system and a system with impurity concentration $p = 0.2$. System size is $L = 1000$.

the literature [14]. In contrast, in the dirty system, the density increases much more slowly with $\lambda$ after crossing the clean critical point. This suggests either a critical point with a very large exponent $\beta$ or exponential behavior.

Let us now investigate the behavior of the dirty system in the low-density tail more closely. In figure 2.5, we plot $\ln \rho_{st}$ as a function of $(\lambda - \lambda_c^0)^{-d_r \nu_\perp}$ for several impurity concentrations $p$, as suggested by eq. (2.5). The data in the left panel of figure 2.5 show that the density tail is indeed exponential, following the prediction $\ln \rho_{st} = -B(\lambda - \lambda_c^0)^{-d_r \nu_\perp}$ over at least two orders of magnitude in $\rho_{st}$. (The clean 2d spatial correlation length exponent is $\nu_\perp = 0.734$ [37].) Fits of the data to eq. (2.5) are used to determine the decay constants $B$. The right panel of figure 2.5 shows these decays constants as function of $\tilde{p} = -\ln(1-p)$. The dependence is close to linear, as predicted below eq. (2.4) (Slight deviations from the theoretical prediction can

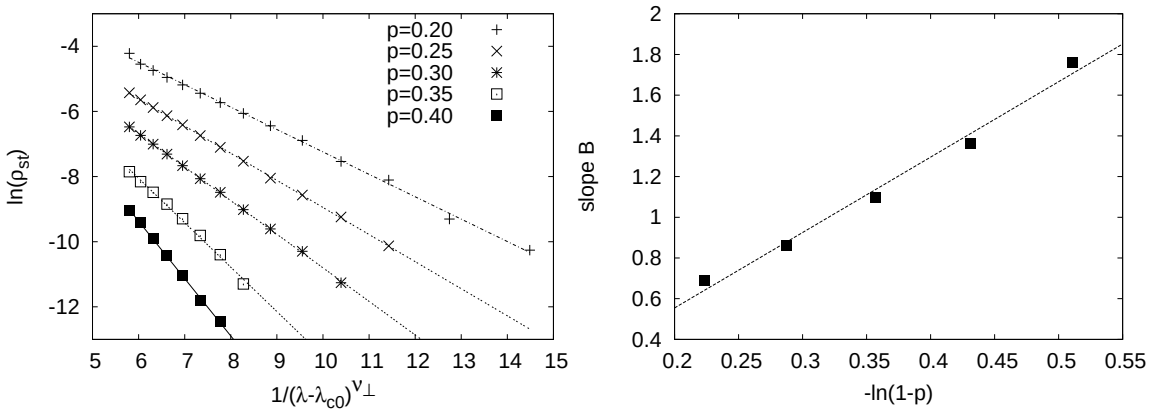


Figure 2.5. Left: Logarithm of the stationary density $\rho_{st}$ as a function of $(\lambda - \lambda_c^0)^{-d_r\nu_\perp} = (\lambda - \lambda_c^0)^{-0.734}$ for several impurity concentrations $p$ and $L = 3000$. The straight lines are fits to eq. (2.5). Right: Decay constant $B$ as a function of $-\ln(1-p)$.

again be attributed to the pre-exponential terms neglected in the extremal statistics theory.)

## 2.5. CONCLUSIONS

To summarize, we have provided extensive numerical evidence that extended impurities destroy the sharp nonequilibrium phase transition in the contact process by smearing and lead to a (nonuniversal) exponential dependence of the density and other quantities on the control parameter. These results are in agreement with the predictions of Ref. [8] which were based on extremal statistics arguments and mean-field theory. In this section, we compare our findings to the more conventional Griffiths effects in the contact process with point-like defects[22, 13], and we discuss general implications for theory and experiment.

Both conventional Griffiths effects and the smearing scenario found in the present paper are caused by rare large spatial regions which are locally in the active phase even if the bulk system is not. The difference between Griffiths effects and the smearing of the transition is the result of disorder correlations. For point-like defects, i.e.,

uncorrelated disorder, the rare regions are of finite size and cannot undergo a true phase transition. Instead, they fluctuate slowly which gives rise to Griffiths effects. In contrast, if the rare regions are infinite in at least one dimension, a stronger effect occurs: each rare region can independently undergo the phase transition and develop a nonzero steady state density. This leads to a smearing of the global transition.

The smearing mechanism found here relies only on the existence of a true phase transition on an isolated rare region. It should therefore apply not only to the directed percolation universality class, but to an entire family of nonequilibrium universality classes for spreading processes and reaction-diffusion systems. Note that while the presence or absence of smearing is universal in the sense of critical phenomena (it depends on symmetries and dimensionality only), the functional form of the density and other observables is *not* universal, it depends on the details of the disorder distribution [27].

Smearing phenomena similar to the one found here can also occur at equilibrium phase transitions. At quantum phase transitions in itinerant electron systems, even point-like impurities can lead to smearing [23] (the necessary disorder correlations are in imaginary time direction). In contrast, for the classical Ising (Heisenberg) universality class, the impurities have to be at least 2d (3d) for the transition to be smeared which makes the phenomenon less likely to be observed [27].

In the context of our findings it is worth noting that, despite its ubiquity in theory and simulations, clearcut experimental realizations of the directed percolation universality class are strangely lacking [11]. To the best of our knowledge, the only verification so far has been found in the spatio-temporal intermittency in ferrofluidic spikes [38]. We suggest that the disorder-induced smearing found in the present paper may explain the striking absence of directed percolation scaling [11] in at least some of the experiments.

We thank R. Sknepnek and U. Täuber for stimulating discussions. We acknowledge support from the NSF under grant No. DMR-0339147. Part of this work has been performed at the Aspen Center for Physics.

# 3. POINT-LIKE DISORDER IN A CONTACT PROCESS

In the previous section, the infinite nature of the rare regions allowed for independent ordering, and thus a smearing of the phase transition. In contrast, the situation for point-like disorder is more conventional, but in a sense more difficult to analyze. As mentioned in Section 1.2, initial renormalization group (RG) methods and simulations achieved very little insight into the nature and structure of this system, producing runaway solutions, and non-universal behavior[13, 14, 15, 16]. Recently, works by Igloi and collaborators[9] have indicated that for point-like disorder, the traditional power law scaling $\xi_{\parallel} \sim \xi_{\perp}^{z}$ is replaced by activated scaling $\xi_{\parallel} \sim \exp(\xi_{\perp}^{\mu})$. As a result, the scaling relationships of time dependent quantities are also modified at the dirty critical point. The new scaling laws have logarithmic dependence of the form

$$\begin{aligned} P_s(t) &\sim (\ln t)^{-\delta} \\ \rho(t) &\sim (\ln t)^{-\delta} \\ N(t) &\sim (\ln t)^{\theta} \end{aligned} \tag{3.1}$$

rather than the power law forms of equation (1.5) (Igloi et al use $\theta$ and $\nu$ for the quantities previously denoted as $\delta$ and $\theta$ respectively). $\delta$ and $\theta$ here are also not the exponents of the clean system but rather ones modified for the dirty system: Igloi et al[9] predict $\delta = 0.38197$ and $\theta = 0.75151$. These logarithmic scaling laws were derived by mapping the system onto a quantum Hamiltonian[34, 36], which led itself to solution[21] via a real space renormalization group (RG) method, originally introduced by Ma, Dasgupta, and Hu[35]. This procedure is possible because the infinite disorder fixed points of the system ensures that the distribution of the random parameters broadens without limit at those points, making the RG treatment asymptotically exact.

These above methods, and thus the predictions they provide, are only valid for large disorder cases; for weak disorder ($c$ close to 1 and/or $p$ close to 0) [9] predicts non-universal power law behavior of the form (1.5) with exponents $\delta$ and $\theta$ that are not constants but depend on the disorder strength $c$ and concentration $p$.

In addition, the Griffiths effects discussed in the Introduction should be valid for the region $\lambda_c < \lambda < \lambda_c^0$, with the power law scaling as in the clean case, though with non-universal exponents that depend on how far into the Griffiths region the system is[14, 13]

In light of the above predictions in the liturature, three questions naturally follow. 1) Is there any numerical evidence of an infinite randomness fixed point? 2) What is the real nature of the critical behavior, and is it true that in the long term limit (asymptotic behavior) the behavior is universal? 3) Is there evidence for the Griffiths effects within the assumed Griffiths region? The goal of the simulations performed is to show that the answer to all three of these questions is, in fact, yes.

## 3.1. SIMULATIONS AND RESULTS

The $1D$ contact process has been simulated using the algorithm described in the first section with linear system sizes ranging from $L = 10^3$ to $10^7$, disorder concentration $p = 0.2$ to 0.5, and disorder strength $c = 0.2$. All quantities recorded are averages over 200 disorder realizations.

The first behavior to be analyzed is the behavior of the disordered system at the clean critical point $\lambda_c^0$. Because this is the value where the clean system is on the cusp between order and disorder, so no region can truly order, or fail to order, the fact that the rare regions are of infinite size in the correlated disorder case, and of finite size in the point-like disordered case cannot matter, since the rare regions exhibit the same behavior as the clean case, i.e. they fail to ever become truly static. Due to this fact, the system cannot distinguish between the two disorder cases. Following

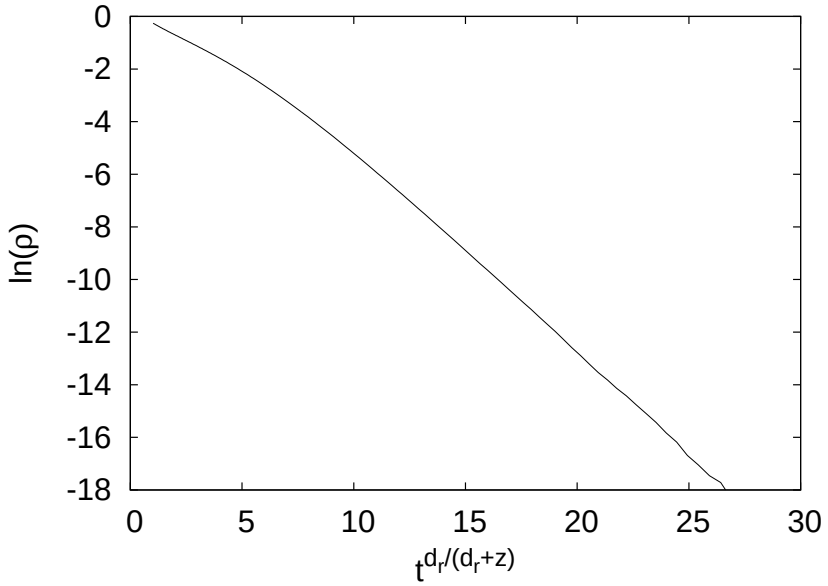


Figure 3.1. Logarithm of the density at the clean critical point $\lambda_c^0 = 3.298$ as a function of $t^{d_r/(d_r+z)} = t^{0.3875}$ for $p = 0.3$, $c = 0.2$ and $L = 2 * 10^7$. The long-time behavior follows a stretched exponential $\ln \rho = -Et^{0.3875}$.

the same arguments as in Section 2, the behavior expected is that of equation (2.8), with the $1d$ rather than the $2d$ value of $z$. Figure 3.1 illustrates that this is indeed the case.

The next question to be addressed was that of the universality of the behavior at the dirty phase transition. Current techniques do not allow a calculation of $\lambda_c$ from known parameters, however upper and lower bounds are easily established. The lower bound for $\lambda_c$ is $\lambda_c^0$, and an upper bound is the first value of $\lambda$ for which a stationary density $\rho_{st} > 0$ can be established. Sampling over $\lambda$ values between these two bounds, and looking for the expected scaling behavior will give the value of $\lambda_c$ for the particular parameter set used. The expected scaling, as derived from Igloi[9] is $\ln(t) \sim \rho^{-1/\delta}$ to exponential accuracy(see equation (3.1)). There will be a $p$ dependent prefactor, but $-1/\delta$ itself should be universal. Figure 3.2 illustrates how the behavior of the system for $p = 0.3$ and $c = 0.2$ changes as a function of $\lambda$. It shows $\rho^{-1/\delta}$ with

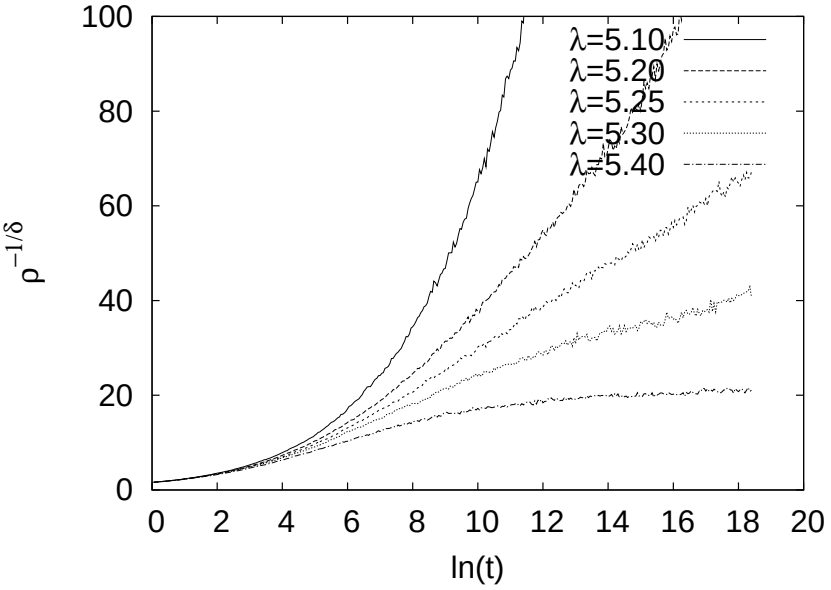


Figure 3.2. Finding $\lambda_c$: $\rho^{-1/\delta} = \rho^{-2.618}$ as a function of the logarithm of time, for $p = 0.3$ $c = 0.2$ and $L = 1 * 10^3$. The straight line $\lambda \approx 5.25$ is $\lambda_c$.

the expected value of $\delta$ as a function of $\ln t$. Where the curve turns up in the plot, the system is subcritical. Where the curve turns down, the system is supercritical. The $\lambda$ value for which the line remains straight at large $t$ is the critical case, $\lambda = \lambda_c$. Figure 3.3 shows the critical cases for several values of $p$. All curves are straight lines for large $t$, thus, the power $-1/\delta$ is indeed universal, though the prefactor is not. Why this differs from Igloi's and Dickman's simulations can be answered by looking at the time scale for which the asymptotic behavior starts to become valid. Both Igloi and Dickman stopped their simulations at $t \approx 10^5$, i.e. $\ln t \approx 11$, but as the graph shows, this is just when the universal behavior is starting to emerge. The apparent contradiction is thus explained.

While graphs are only provided for the case of varying impurity concentration $p$, simulations are currently being performed to investigate the effects of variations in the impurity strength $c$. Igloi claimed universality for strong disorder cases, and even in the case of the small $p$, it could be argued that despite the rare nature of the

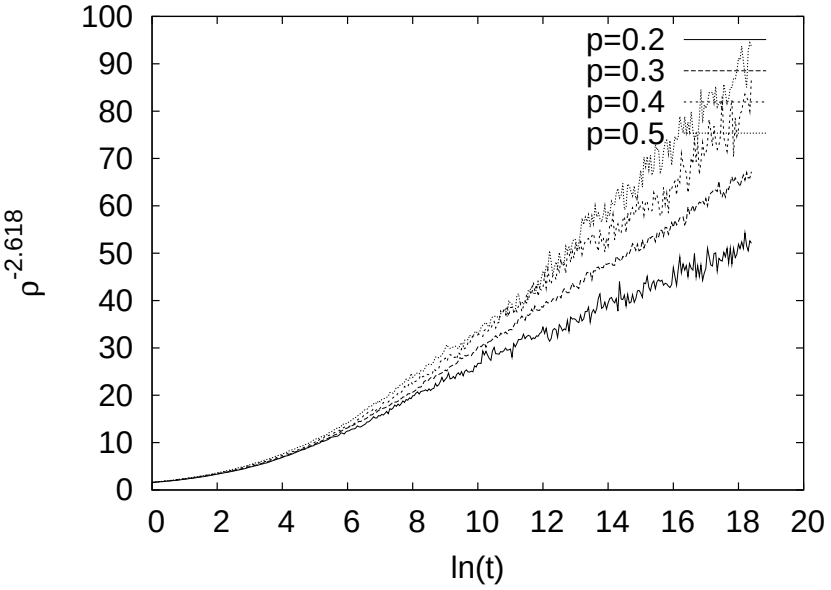


Figure 3.3. $\rho^{-1/\delta} = \rho^{-2.618}$ as a function of the logarithm of time, for $p = 0.2, \ldots, 0.5$ $c = 0.2$ and $L = 1 * 10^3$. The exponent is universal, though there are non-universal prefactors.

disordered points, the strength of them keeps this in the realm of strong disorder. Simulations with $c = 0.4$ and $c = 0.6$ have already been performed, and show no qualitative differences from the $c = 0.2$ shown here. Runs with $c = 0.8$ are currently in progress, and should they continue the trend, as seems likely, this should firmly set to rest any questions of universal behavior only being valid for strong disorder.

As somewhat of an aside, Figure 3.4 illustrates the expected behaviors of $P_s(t)$ and $N(t)$. The left panel plots $P_s(t)$ in analogous form as $\rho(t)$ in Figures 3.2 and 3.3. At long time the curve is a straight line, showing the agreement with the predicted form. The right panel shows the number of sites of a surviving cluster, which can be expressed as $N(t)/P_s(t) \sim (\ln t)^{\theta+\delta}$.

Lastly, the question of Griffiths effects remains to be addressed. In this region between $\lambda_c$ and $\lambda_c^0$ we expect behavior of the form $\rho(t) \sim t^x$ where $x$ is a function of $(\lambda - \lambda_c^0)$. Figure 3.5 illustrates that behavior.

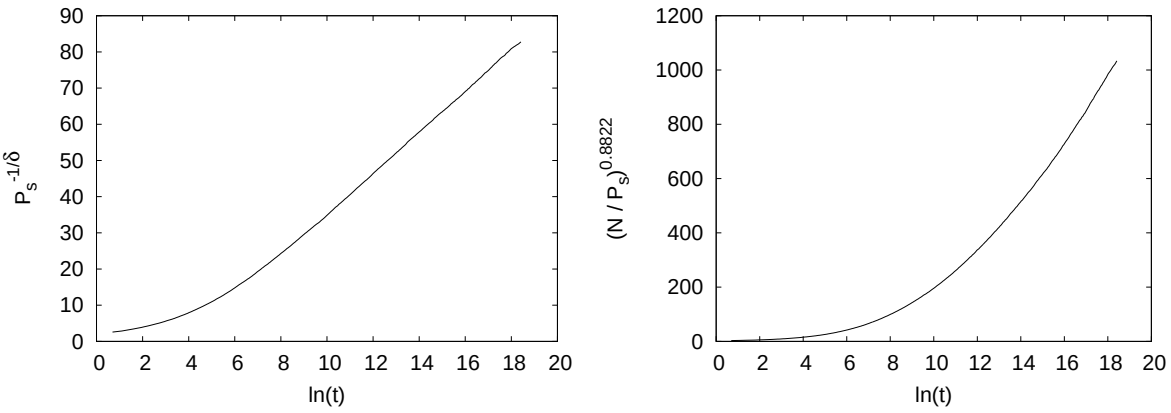


Figure 3.4. Left:$P_s^{-1/\delta} = P_s^{-2.618}$ as a function of the logarithm of time, for $p = 0.3$ $c = 0.2$ $L = 1 * 10^6$ and $\lambda = \lambda_c$ Right:$(N/P_s)^{1/(\delta+\theta)} = (N/P_s)^{0.8822}$ as a function of the logarithm of time, for $p = 0.3$ $c = 0.2$ $L = 1 * 10^6$ and $\lambda = \lambda_c$. The inclusion of $P_s$ and $\delta$ were necessary due to the way $N$ was calculated(see text)

## 3.2. CONCLUSIONS

Hopefully the graphs and short explanations above have answered the questions asked above. As seen in the Figure 3.2 the $1d$ contact process exhibits activated scaling at the clean critical point, in accordance with the predicted form. This demonstrates the presence of an infinite randomness fixed point, of the sort discussed throughout this paper. The scaling of the system for different values of $c$ and $p$ was shown to be universal, in contrast with prior predictions, and the extremely slow dynamics of the system have been offered as an explanation of this discrepancy. Lastly the scaling behavior in the region between $\lambda_c$ and $\lambda_c^0$ was examined, and power laws with non-universal exponents were shown, establishing that region as a Griffiths region.

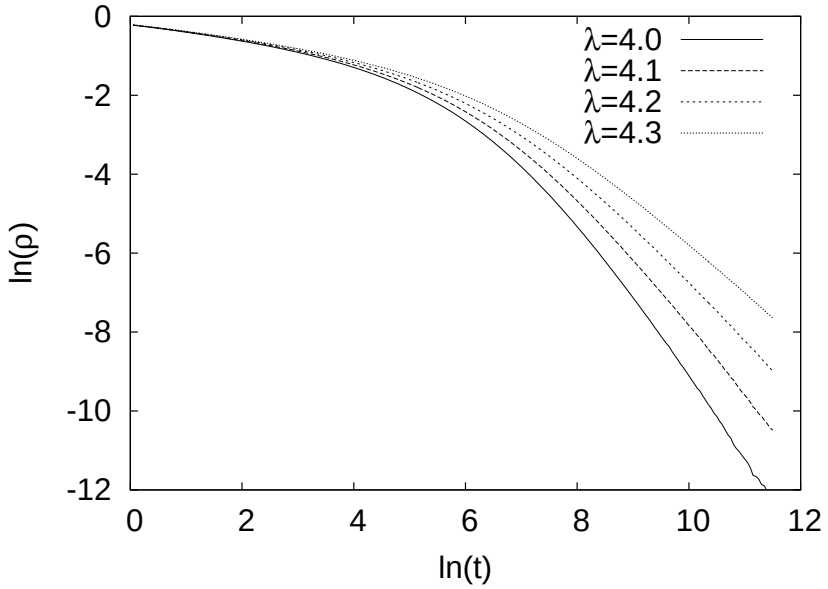


Figure 3.5. Logarithm of the density for selected values of $\lambda$ in the Griffiths region ($3.298 < \lambda < 5.24$) as a function of $\ln t$ for $p = 0.3$, $c = 0.2$ and $L = 2{*}10^7$. Non-universal power law behavior can be seen.

# 4. CONCLUSIONS

To summarize, Monte-Carlo simulations of the 1d and 2d contact process have provided extensive numerical evidence that extended impurities destroy the sharp nonequilibrium phase transition in the contact process by smearing and lead to a (nonuniversal) exponential dependence of the density and other quantities on the control parameter. These results are in agreement with the predictions of Ref. [8] which were based on extremal statistics arguments and mean-field theory. In contrast, point-like defects retain the sharp phase transition, but with activated dynamical scaling, as predicted by the Renormalization Group solved in Ref [9], where an infinite-randomness fixed point was found. However in contrast to the predictions of this reference, no evidence was found for non-universal behavior. At sufficiently long times the critical behavior is universal for all disorder strengths.

Both conventional Griffiths effects and smearing are caused by rare large spatial regions which are locally in the active phase even if the bulk system is not. The difference between Griffiths effects and the smearing of the transition is the result of disorder correlations. For point-like defects, i.e., uncorrelated disorder, the rare regions are of finite size and cannot undergo a true phase transition. Instead, they fluctuate slowly which gives rise to Griffiths effects. In contrast, if the rare regions are infinite in at least one dimension, a stronger effect occurs: each rare region can independently undergo the phase transition and develop a nonzero steady state density. This leads to a smearing of the global transition.

In the context of these findings it is worth noting that, despite its ubiquity in theory and simulations, clearcut experimental realizations of the directed percolation universality class are strangely lacking[11]. It is suggested that the disorder-induced smearing or the activated scaling of the infinite randomness critical point found in

this paper may explain the striking absence of directed percolation scaling in at least some of the experiments.

# APPENDIX A.

# PROGRAMMING IMPLEMENTATION AND SOURCE CODE

It is useful to consider the exact implementation of the simulation used to generate the results presented before, in the interests of confirmation and reproducibility.

The code was run in a parallel environment controlled by MPI. Each machine set up an independent lattice field, starting from a full site, and evolved the system according to random numbers generated from a specified starting seed, which was sequentially assigned to the involved machines. This allowed reproducible results, while still allowing for each run to proceed independently of the others.

The dynamical quantities kept by the system consisted of the following: A list of each site ordered by cartesian coordinates, and containing the occupancy status of the site, as well as whether it was a disorder site or not. A separate list of all occupied sites, in no particular order, used for random selection purposes. The number of occupied sites $N_p$, the time $t$, and the next expected output time. Static quantities kept by the system were the dimensionality, the values of $\lambda$ $p$ and $c$, the size of the system, the total time of the simulation, the seed used for the RNG, the number of computers participating in the parallel system, the individual machines place within that group of computers, and the total number of realizations to perform.

At any given point in time each site is associated with either a 0, representing an unoccupied site, or a 1, representing an occupied site. The system is allowed to evolve in time by picking a single occupied site from the list of them at random, and selecting either creation, at probability $\lambda(\vec{r})/(\lambda(\vec{r})+1)$ or annihilation at probability $1/(\lambda(\vec{r})+1)$, where $\lambda(\vec{r})$ is the value of the control parameter at the originating site. If creation is selected, one of the $2d$ nearest neighbors is selected at random, and its value is examined. If it is unoccupied, its value is set to 1, and $N_p$ is incremented, otherwise nothing happens. If annihilation is selected, the chosen site's value is set to 0. In all of these cases, time is then advanced by $1/N_p$, where $N_p$ is the total number of infected individuals. The time is then compared to the next expected output time, and if it meets or exceeds it, the value is recorded in the output array. Because of the needed discretization, and the random nature of the evolution of $N_p$ the recorded values for different systems will not always have identical time stamps, but they will be very close, compared to the time scales of interest. To illustrate this, consider that at small values of $t$ where these differences would be most apparent, $N_p$ will be very large, and thus $\Delta t$ will be small compared to $t$, as $t$ increases, the dynamics

of the system slow down, and the larger variance in $t$ matters comparatively less. Lastly, $t$ and $N_p$ are compared to the exit conditions, namely $t > t_{max}$ and $N_p = 0$. If they aren't met, the whole procedure repeats itself and if so, the system ends the realization, and starts the next (if needed). At the end of all realizations, the system collects all of the values, and averages them together, the individual values are not kept, but could be if situations required them.

What follows now is the source code used to generate the results in section 3. It differs in a few small ways, and one large way, from the code used for section 2. The first small difference is of course that since it is a $1d$ version, all of the information on the sites that were occupied is stored as simple arrays rather than a more complicated struct. Output values are also sampled in logarithmic time, rather than linearly, the larger times required in Section 3 simply resulted in files that were unmanageable if sampled linearly. Lastly some of the orders in which creation/destruction and neighbor selection were changed for greater speed.

The large difference (though some may disagree on how big of a difference it is) is that while the version used for generating the correlated disorder data was written in C++, this is written in old-style C. The reason for this change is that as it became apparently that the pointlike disorder realizations were going to require much more extensive simulations, optimization of code became more of a concern. When the time scale of the C++ code was compared to some reference F90 code written by Thomas Vojta, a factor of 5 difference was quickly noticed. After some optimizations to make the C++ code's structure identical to that of the F90 code, a factor of 3 speed difference was still evident, much larger than the 10-15% advantage typically accepted as normal within the community. Several different compilers were tried, as well as larger runs, establishing that this was A) indeed a multiplicative, rather than an additive difference, and B) that it was not an oddity of a particular complier.

As an experiment, the C++ wrapper was removed from the RNG, which was the only C-style incompatible portion of the code, and the speed difference dropped to the accepted 10% margin. This is provided as a cautionary tale to any others involved in computational physics, sometimes almost trivial difference, (such as a simple code wrapper) can have very large performance impacts.

```
#define versionN 2.3.2p
#define dimension 1

/*

Version 2.2.0

    First working version, parallel, 2-D
    Finished 11-2-04

Version 2.3.0
    First working 1-D version

Version 2.3.1
    Bunch of changes, slight speed optimizations
    Switched to logarithmic output in time

Version 2.3.2
    More speed optimizations, switched to straight C
*/



#include <stdio.h>
#include <math.h>
#include "mpi.h"


int MySize; int MyRank;

double rho_final[500]; int occupancy[1000000];  // the occupied
sites array}

char occupied[1000000]; //table of occupied sites
    double P_Compare[1000000];

double rho_array[500]; double time_array[500];

double rho_index[24000]; //for gathering all of the different runs

int num_cycles;

int start_seed;
```

```
int time_max;

int array_size;

int cycle (double, double, double, int, int); double rlfsr113 ();
void lfsrinit(long idum);

int main (int argc, char* argv[]) {
    MPI_Init(&argc,&argv);  //declaring parallell array
    MPI_Comm_rank(MPI_COMM_WORLD, &MyRank);
    MPI_Comm_size(MPI_COMM_WORLD, &MySize);

    int length_d1;  //dimension parameters

    double lambda_min;  //set of lambda parameters
    double lambda_max;
    double lambda_step;

    double dilution;  //set of impurity parameters
    double impurity_strength;

    FILE* iFile;

        iFile = fopen("input1d.txt","rt"); //input parameter file

        fscanf (iFile, " %i",&num_cycles); //defining global values
        fscanf (iFile, " %i",&start_seed);
        fscanf (iFile, " %i",&time_max);

        fscanf (iFile, " %i",&length_d1); //reading in local values
        fscanf (iFile, " %lf",&lambda_min);
        fscanf (iFile, " %lf",&lambda_max);
        fscanf (iFile, " %lf",&lambda_step);
        fscanf (iFile, " %lf",&dilution);
        fscanf (iFile, " %lf",&impurity_strength);

    fclose(iFile);

    double lambda_current=lambda_min;
    int num_runs = num_cycles/MySize;
    array_size=20*log(time_max)+1;

    while ( lambda_current < lambda_max)
        {
            for (int count = 0; count < num_runs; count++)
```

```
            {
            int seed=start_seed+(count*MySize)+MyRank;
            cycle(lambda_current,dilution,impurity_strength,length_d1,seed);
            }
            lambda_current+=lambda_step;
    }


    MPI_Finalize();
    return 0;
}


int cycle (double lambda, double P, double C, int d1, int seed) {
    double lambda_weak = lambda * C;
    double P_Strong = lambda / (1 + lambda);
    double P_Weak = lambda_weak / ( 1 + lambda_weak );
    int N = 0;  //number of occupied sites

    lfsrinit(seed);  //initialize random number generator

    //generate a random arrangement of diluted sites
    for (int a=0; a <d1; a++ )
        {
            if (rlfsr113() <P)
            {
                P_Compare[a] = P_Weak;
            }
            else
            {
                P_Compare[a] = P_Strong;
            }
            occupied[a] = 1;
        }

        for (int c=0; c < d1; c++) //initializing all sites to occupied
        {
            occupancy[N]=c;
            N++;
        }

        int save_count=0;
        double save_time=1.0;
        double time = 0;
```

```
double time_count=1.0;
for (int aa=0; aa<500; aa++)
{
    time_array[aa]= time_count;
    time_count*=1.0512710963;
    rho_array[aa]= 0;
}

while (time < time_max && N>0)
{
//samples a small set of data points to save file space
    if (time>save_time)
    {

        rho_array[save_count] = (N*1.0)/(d1);
        //time_array[save_count] = save_time;
        save_time*=1.0512710963;
        save_count++;
    }

    time += (1.0 / N);


    int select = N * rlfsr113();  //picking a random site

    int x = occupancy[select];

    int x_step=0;

    int new_x=x;

    if ( rlfsr113() > P_Compare[x]) //destruction
    {
        occupied[x] = 0;
        occupancy[select]=occupancy[N-1];
        N--;
    }

    else
    {
        if ( rlfsr113() < .5)  //picking left or right neighbor
        {
            new_x++;
            if (new_x==d1)
            {
```

```
                    new_x=0;
                }
            }
            else
            {
                new_x--;
                if (new_x==-1)
                {
                    new_x=d1-1;
                }
            }

            if ( occupied[new_x]==0 ) //creation
            {
                occupied[new_x] = 1;
                N++;
                occupancy[N-1] = new_x;
            }
        }

    }

//only if its the root machine do we do anything with rho_index
if (MyRank==0)
{
    for (int a=0; a<24000; a++)
    {
        rho_index[a]=0;
    }
}
//if this is the first run for this machine, initialize output to zeros
if ( (seed - start_seed)%num_cycles == 0)
{
    for (int a=0; a<500; a++)
    {
        rho_final[a]=0;
    }
}

//collect all of the individual runs
MPI_Gather (rho_array,500,MPI_DOUBLE,rho_index,500,
            MPI_DOUBLE,0,MPI_COMM_WORLD);
```

```
char filename[100];  //declaring file output information
sprintf(filename, "lambda=%lf_P=%lf_C=%lf_size=%i.txt", lambda, P,C, d1);
FILE* oFile;
oFile = fopen(filename, "wt");

if (MyRank==0)  //only if its the root machine do we store values
{
    for (int a=0; a<array_size; a++) //going over each of the time steps
    {
        int index=0;
        rho_array[a]=0;
        while (index<MySize)
        {
            //summing up all of the values at each time step
            rho_array[a]+= rho_index[a+(index*500)];
            index++;
        }
        //dividing by total number of values to get answer
        rho_final[a]+=rho_array[a]/num_cycles;
    }
}


// if this is the last cycle for the root machine
if ( seed - start_seed == num_cycles-MySize)
{
    // a lot of heading
    fprintf (oFile, "#Created with version versionN \n");
    fprintf (oFile, "#Parameters are lambda = %lf, array dimension = %i,
        seeds = %i to %i \n",lambda,d1,seed + MySize - num_cycles,
        seed+MySize-1);
    fprintf (oFile, "#Dilution(p) = %lf, Lambda reduction(c) = %lf\n",P,C);
    fprintf (oFile, "#Time\tRho\t\t\n");
    // old format
    //fprintf (oFile, "#SaveCount %i, N%i, time %lf time_max %i\n",
    //  save_count, N, time, time_max);

    for (int output = 0; output<500; output++)
    {
        if (rho_final[output]>0)  //don't output zero lines.
        {
            fprintf (oFile, "%lf\t%lf\n", time_array[output],
                rho_final[output]);
        }
    }
```

```
    }

    fclose (oFile);

    return 0;
}

//random number generator starts here, I didn't write it so I can't
comment on it.

#define IA 16807 #define IM 2147483647 #define IQ 127773
    #define IR 2836

unsigned long z1, z2, z3, z4;

double rlfsr113 ()
   {
   unsigned long b;
   b  = (((z1 << 6) ^ z1) >> 13);
   z1 = (((z1 & 4294967294) << 18) ^b);
   b  = (((z2 << 2) ^ z2) >> 27);
   z2 = (((z2 & 4294967288) << 2) ^b);
   b  = (((z3 << 13) ^ z3) >> 21);
   z3 = (((z3 & 4294967280) << 7) ^b);
   b  = (((z4 << 3) ^ z4) >> 12);
   z4 = (((z4 & 4294967168) << 13) ^b);
   return((z1 ^ z2 ^ z3 ^ z4 ) * 2.3283064365e-10);
   }

void lfsrinit(long idum)
   {
   long k;
   double d;
   if (idum <= 0) idum = 1;
   k=(idum)/IQ;
   idum=IA*(idum-k*IQ)-IR*k;
   if (idum < 0) idum += IM;
   if (idum < 2) z1=idum+2; else z1=idum;
   k=(idum)/IQ;
   idum=IA*(idum-k*IQ)-IR*k;
   if (idum < 0) idum += IM;
   if (idum < 8) z2=idum+8; else z2=idum;
   k=(idum)/IQ;
   idum=IA*(idum-k*IQ)-IR*k;
   if (idum < 0) idum += IM;
```

```
if (idum < 16) z3=idum+16; else z3=idum;
k=(idum)/IQ;
idum=IA*(idum-k*IQ)-IR*k;
if (idum < 0) idum += IM;
if (idum < 128) z4=idum+128; else z4=idum;

d=rlfsr113();
}
```

# BIBLIOGRAPHY


[1] Hinrichsen H 2000 *Adv. Phys.* **49** 815

[2] Chopard B and Droz M 1998 *Cellular Automaton Modeling of Physical Systems* (Cambridge University Press, Cambridge, England).

[3] Marro J and Dickman R 1999 *Nonequilibrium Phase Transitions in Lattice Models* (Cambridge University Press, Cambridge, England).

[4] Täuber U C 2003 *Adv. in Solid State Phys.* **43** 659

[5] Grassberger P and de la Torre A 1979 *Ann. Phys. (NY)* **122** 373

[6] Liggett T 1985 Interacting Particle Systems (Springer-Verlag). pp 265-314

[7] Goldenfeld N 1992 *Lectures On Phase Transitions And The Renormalization Group* (Westview Press, Cambridge MA)

[8] Vojta T 2004 *Phys. Rev. E* **70**

[9] Hooyberghs J, Igloi F and Vanderzande C 2003 *Phys. Rev. Lett.* **90** 100601

Hooyberghs J, Igloi F and Vanderzande C 2004 eprint cond-mat/0402086

[10] Dickman R 1999 *Phys. Rev. E* **60** R2441

[11] Hinrichsen H 2000 *Braz. J. Phys.* **30** 69

[12] Janssen H K 1997 *Phys. Rev. E* **55** 6253

[13] Noest A J 1986 *Phys. Rev. Lett.* **57** 90

[14] Moreira A G and Dickman R 1996 *Phys. Rev. E* **54** R3090

[15] Bramson B, Durrett R Schonmann R H 1991 *Ann. Prob.* **19** 960

[16] Cafiero R, Gabrielli A and Muñoz M A 1998 *Phys. Rev. E* **57** 5060

[17] Harris A B 1974 *J. Phys. C* **7** 1671

[18] Motrunich O, Mau S-C, Huse D A, and Fisher D S, 2000 *Phys. Rev. B* **61** 1160

[19] Aharony A and Harris A B 1996 *Phys. Rev. Lett.* **77** 3700

[20] Wiseman S and Domany E 1998 *Phys. Rev. Lett.* **81** 22

[21] Fisher D S 1992 *Phys. Rev. Lett.* **69** 534; 1995 *Phys. Rev. B* **51** 6411

[22] Griffiths R B 1969 *Phys. Rev. Lett.* **23** 17

[23] Vojta T 2003 *Phys. Rev. Lett.* **90** 107202

[24] Skepnek R and Vojta T 2004 *Phys. Stat. Sol.(b)* **241** 2118

[25] Fisher D S 1995 *Phys. Rev. B* **51** 6411

[26] McCoy B M and Wu T T 1968 *Phys. Rev. Lett.* **23** 383 (1968)

McCoy B M and Wu T T 1968 *Phys. Rev.* **176** 631

[27] Vojta T 2003 *J. Phys. A* **36** 10921

[28] Janssen H K 1981 *Z. Phys. B* **42** 151

Grassberger P 1982 *Z. Phys. B* **47** 365

[29] Harris T E 1974 *Ann. Prob.* **2** 969

[30] Ziff R M, Gulari E, and Barshad Y 1986 *Phys. Rev. Lett.* **56** 2553

[31] Tang L H and Leschhorn H 1992 *Phys. Rev. A* **45** R8309

[32] Pomeau Y *Physica D* **23** 3

[33] Webman T et al. 1998 *Phil. Mag. B* **77** 1401

[34] Alcaraz F C 1994 *Ann. Phys. (NY)* **230** 250

[35] Ma S K, Dasgupta C and Hu C-K 1979 *Phys. Rev. Lett.* **43** 1434; Dasgupta C and Ma S K 1980 *Phys. Rev. B* **22** 1305

[36] Schutz G M 2000 in *Phase transitions and critical phenomena*, edited by C. Domb and J.L. Lebowitz (Academic, London), Vol. 19.

[37] Voigt C A and Ziff R M 1997 *Phys. Rev. E* **56** R6241

[38] Rupp P, Richter R and Rehberg I *Phys. Rev. E* **67** 036209

# VITA

Mark Edward Dickison was born in the KU Medical Center on March 5th 1981. He received his Bachelor's of Science in the subject of Physics from the University of Missouri Rolla in 2003. Since then he has been working as a graduate research assistant to Dr. Thomas Vojta.